Macromolecules

Article

pubs.acs.org/Macromolecules

One-Pot Thermo-Remendable Shape Memory Polyurethanes

Guadalupe Rivero,[†,‡] Le-Thu T. Nguyen,[†,§] Xander K. D. Hillewaere,[†] and Filip E. Du Prez*[,†]

[†]Polymer Chemistry Research Group, Department of Organic Chemistry, Ghent University, Krijgslaan 281 S4 bis, Ghent, Belgium

[‡]Instituto de Investigaciones en Ciencia y Tecnología de Materiales (INTEMA), Universidad Nacional de Mar del Plata, Mar del Plata, Argentina

Supporting Information

ABSTRACT: Furan-based thermoset polyurethanes have been prepared in a one-pot fashion with the ability to self-mend under mild temperature conditions, by making use of a Diels–Alder shape-memory assisted self-healing (DASMASH) approach. For this, thermoreversible covalent bonds, obtained by Diels–Alder chemistry, are introduced as cross-linkers into a polycaprolactone (PCL) containing polyurethane material. It is demonstrated that, after introduction of a crack into the PU-thermoset, Diels–Alder bonds preferentially break, regenerating free furan/maleimide functional groups, while the shape memory effect favors the crack closure at temperatures above the melting point of PCL, simultaneously resulting in a reformation of the reversible cross-links. The reversibility and shape memory ability of the materials were optimized and studied by FTIR, ^{1}H NMR and tensile measurements. Different compositions were used to properly understand the role and influence of each component. The polyurethane materials healed at 50 °C after mechanical damage induced by either the application of a large tensile deformation or by performing controlled macro/micro scratches with a depth sensing indenter. Online FT-IR monitoring provided a kinetic description of the system reversibility for numerous cycles. Furthermore, mechanical recovery with complete disappearance of the microscratches was accomplished after multiple cycles of large tensile deformation. The results were not only confirmed by an optical inspection and scanning electron microscopy, but also with confocal microscopic mapping, by comparison of the cross-section profiles of the microscratches before and after healing.

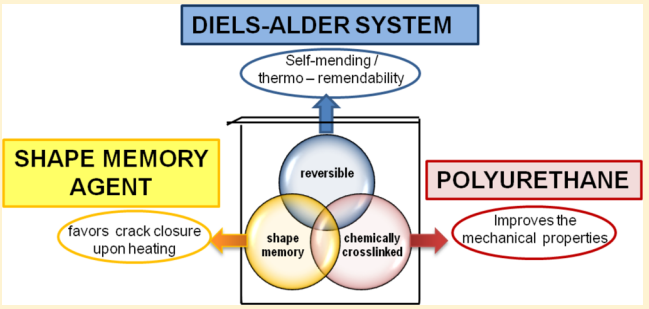

INTRODUCTION

The extension of materials service lifetime is one of the main challenges of science in the past decade. A polymer material with self-mending capability not only provides comfort to the customer, but also reduces energy, resources and waste. Several approaches have included external healing agents that act in case of damage.[1−3] On the other hand, reversible chemical reactions have been exploited in recyclable systems for reconstruction of the structures.[1,4−10] In this respect, Diels–Alder (DA) concerted cycloaddition reactions have been much investigated because of their reversible response to an external stimulus.[1,3,11] On the basis of this feature, many research groups have intended to achieve self-healing and/or recyclable materials.[12−14]

Since the first contribution of Chen et al.[11,15] regarding the use of Diels–Alder chemistry in remendable materials, several systems aimed to improve the performance of systems based on adducts reformation. The first main strategy made use of multifuran/maleimide moieties[11] that resulted in a reversible network. Despite the covalent nature of DA adducts bonds, the involved bond strength is much lower than for other available covalent bonds. As a consequence, when a fissure appears, these weaker bonds would first cleave by the retro DA reaction, in order to allow the crack to propagate.[11] Later on, other authors[16] attached furan/maleimide functionalities as pendant groups to epoxy-based systems, evidencing some material recyclability at temperatures above 100 °C. Besides, self-healing properties were qualitatively reported by optical images in a thermoset epoxy polymer containing Diels–Alder adducts.[17] Gaina et al.[18] prepared polyurethanes by a Diels–Alder reaction between urethane-bismaleimides and bifuryl monomers. In general, the challenges ahead are oriented to provide direct proofs of remendability and accurate quantification of the healing efficiency.

Besides, shape memory polymers (SMPs) are widely applied for engineering applications because of the capability of recovering their original shape by heating. Among the shape-memory polyurethanes reported, those containing covalent cross-links demonstrated better recovery ratios and shape fixity.[19,20] The techniques for cross-linking included post-polymerization melting,[19] incorporation of hyperbranched polymers,[20] etc. Preparation techniques have been optimized to link the structure to the shape memory properties in a controlled way.[21,22]

Polycaprolactone (PCL) is a linear semicrystalline polymer with a low glass transition temperature, often used as a shape

Received: December 3, 2013
Revised: February 25, 2014

   dx.doi.org/10.1021/ma402471c | Macromolecules XXXX, XXX, XXX–XXX

memory agent because of its sharp transition temperature range. After incorporating furan/maleimide moieties, the Diels–Alder reaction has been used for the preparation of several networks based on PCL.[23−26] Some of them have reported recyclability properties.

Rodriguez et al.[27] have introduced the term "shape memory assisted self-healing" (SMASH) for a strategy originally applied in a linear/cross-linked PCL blend. The plastic deformation recovery assists to close the cracks, so that linear chains are able to diffuse and re-entangle the free surfaces. Damage was healed by heating above the melting temperature (T_m) of the linear PCL in an efficient and cyclic way. However, the incorporation of a mechanical support was mandatory for its usage. The same group recently applied this combined strategy in a two-step preparation of coatings formed by an epoxy matrix containing electrospun PCL fibers.[28] By means of a heating procedure, a shape memory effect brings together the crack surfaces, while the melting and flow of PCL fibers are responsible for the rebonding. In this case, mechanical recovery was not shown, but the closure of the crack was accomplished to restore the functional corrosion resistance.

The main objective of our approach aims to tune the functionality of polymeric materials under mild conditions, both from a structural and functional point of view. In our concept, the shape memory effect only promotes the contact of damaged surfaces, but it is not providing the main basis of the healing approach as we also intended to restore the chemical structure at the crack interface. In fact, the healing strategy applied for polyurethane materials in this research, is based on a synergetic combination of Diels–Alder covalent thermo-remendability with the simultaneous assistance of a shape memory agent to favor the crack closure, as schematically depicted in Figure 1. In this way, the concept can be denoted as "Diels Alder based shape memory assisted self-healing" (DASMASH).

Second, this work focuses on obtaining a material with good mechanical properties and structural integrity as main practical features, by the introduction of permanent cross-links on top of the reversible ones. The preparation methods were optimized in such a way that the synthesis can be performed in a one-pot fashion. This protocol would bring simplicity to potential industrial processes. Moreover, compositions were tuned to have the remendability temperature close to the usage temperatures, without losing the mechanical integrity.

In our protocol, an initial Diels–Alder reaction between a bis-maleimide and a furan functionalized diol accomplishes a double function: on one hand the introduction of thermo-reversible moieties (Diels–Alder adducts) as cross-linkers, while on the other hand providing a part of the required hydroxyl functional groups for the subsequent polymerization.

It will be demonstrated that the proposed material design combines the main advantages of several cutting edge topics in a complex functional system, but achievable in a straightforward, one-step process.

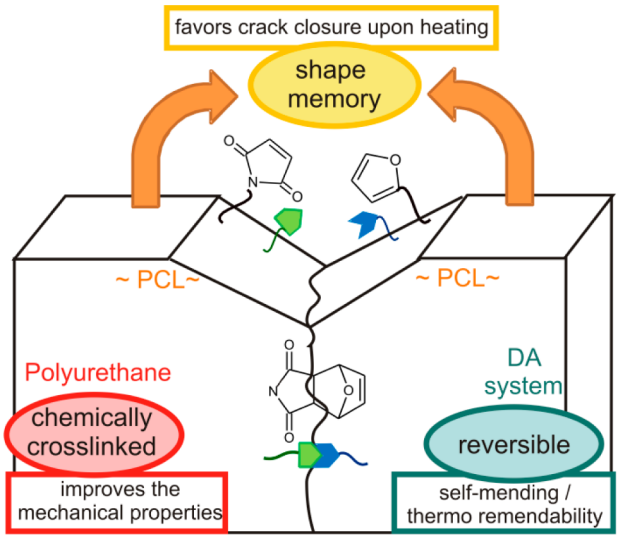

Figure 1. Schematic depiction of the Diels–Alder based shape memory assisted self-healing process in a polyurethane material based on PCL and furan-maleimide chemistry.

EXPERIMENTAL SECTION

Materials. All materials were used as received, without further purification. Trimethylolpropane monoallyl ether (TMPME), 2-furanmethanethiol (FM), 2,2-dimethoxy 2-phenylacetophenone (DMPA) and 1,1′-(methanediyldibenzene-4,1-diyl)bis(1H-pyrrole-2,5-dione) (bis-maleimide, bM) were purchased from Sigma-Aldrich.

As switching segment and shape memory agent, polycaprolactone diol (PCL, M_w equal to 6000 g/mol) was purchased from Solvay. For the polyurethane synthesis, hexamethylene diisocyanate (HDI), zirconium acteylacetonate (Zr-based catalyst) and dibutyltin dilaurate (Sn-based catalyst) were purchased from Sigma-Aldrich. Tetrahydrofuran (THF) and dimethyl sulfoxide (DMSO), used as solvents, were purchased from Sigma-Aldrich.

Synthesis of Diol with Furan Pendant Moieties. A thiol–ene reaction took place between TMPME (3.5 g, 17.5 mmol) and FM (1.77 mL, 17.5 mmol), in liquid state, in N_2 atmosphere. DMPA photoinitiator (300 mg, 1% mol/total mols) was dissolved in THF (14 mL/total mols) and then added to the reaction mixture. After an overnight exposure to UV light (wavelength of 365 nm, with eight lamps of 9 W circularly oriented), a liquid furan diol (FD) was obtained (288.4 g/mol, yield 92%) (Figure S1, Supporting Information). After the reaction, the solvent was removed in a rotavapor.

Polyurethanes Preparation. All reactants and glasswork were previously dried. In the same reaction vessel containing the furan diol, the bis-maleimide was added in a 1:1 equivalent ratio, under vacuum with constant stirring. A minimal amount of DMSO was used for dissolving the PCL diol. A concentration of 2 equiv/L was used for Diels–Alder reactions at 40 °C. As displayed below, the relative amounts of reactants were varied in order to obtain polyurethanes with different hard segment contents.

Once the Diels–Alder adducts were formed, PCL was dissolved in the reaction mixture at 50 °C. Finally, the catalyst and the HDI reactant were incorporated to initiate the polyurethane formation. The ratio of −NCO/−OH functional groups was fixed to 1.05 in all cases. Vacuum and stirring were maintained to avoid undesirable side reactions with water and to ensure a homogeneous system, until the liquid mixture was injected in molds. Samples were cured overnight at 50 °C, followed by two more days at 60 °C. After opening the molds, the polyurethanes were washed by a Soxhlet extraction in acetone at 60 °C, to eliminate remaining monomers and solvent.

Materials with four different compositions were prepared by varying the hard segment content (HS): 15, 25, 35, and 50%. These values were calculated as the mass percentage of (FD + HDI) with respect to the total sum of (FD + PCL + HDI).

Two different PU catalysts were used and their influence on the final structure and properties was studied. Materials were systematically named as PU-(%HS)-Z or PU-(%HS)-T, for the polyurethanes prepared with Zr (4.8 g of catalyst/mol of HDI) or tin catalyst (6.2 g of catalyst/mol of HDI), respectively.

dx.doi.org/10.1021/ma402471c | Macromolecules XXXX, XXX, XXX−XXX

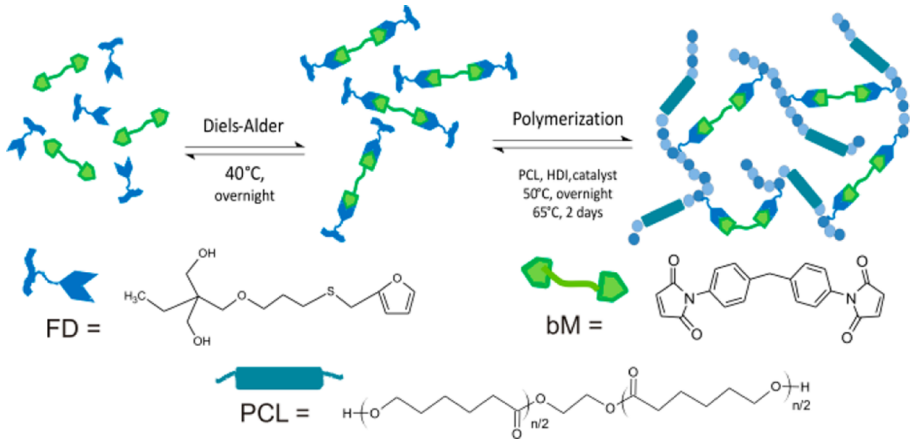

Figure 2. Schematic depiction of the PU preparation procedure.

For comparative purposes in the DA reaction, *N*-methyl maleimide (mM), purchased from Sigma-Aldrich, was used as a non-cross-linked counterpart material.

Structural Analyses. Fourier Transform infrared spectroscopy (FT-IR) was performed on a Mettler Toledo React-IR 4000 equipment, by scanning from 4000 to 600 cm^{-1}. For comparison purposes, the peak intensity was normalized with the aromatic (γ, C=C) peak at 1512 cm^{-1}, which did not modify its intensity during the reaction.

The Diels–Alder reaction was also followed by ^1H NMR on a Bruker Avance Ultrashield, 300 MHz, with deuterated dimethyl sulfoxide as solvent. A kinetic study on the bM and FD reaction was performed at different temperatures: 20, 40, 50, and 60 °C. The peak at δ = 7.54 ppm, assigned to the furan ring, was chosen for conversion calculations, as there was not overlap with any product signal. The retro-DA reaction (rDA) was followed as a function of time in a similar way at 80, 90, 100, and 110 °C. Once the best conditions were determined, at least three cycles were performed.

PU Characterization. Differential scanning calorimetry (DSC) was performed in a cyclic way, from −50 to +180 °C at 10 °C/min under N_2 atmosphere on DSC-1 Mettler Toledo equipment. The first heating curve is not shown. Thermogravimetrical analyses (TGA) were performed from room temperature until 800 °C at 10 °C/min, under N_2 atmosphere with a TGA/SDTA851e equipment. Mechanical properties were measured with a Tinius Olsen H10KT tensile testing machine, making use of a 5000 N load cell. At least six specimens were tested for each composition. Dynamic mechanical analysis (DMA) was performed from −80 to +70 °C, in a TA Instrument (DMA 2980) at 10 °C/min with a frequency of 1 Hz.

Shape Memory and Healing Ability. All samples were subjected to different kinds of mechanical and thermal damage:

- Samples were heated up to 100 °C to partially break the Diels–Alder adducts in the PUs by the rDA reaction. After 1 h, they were cooled down to 50 °C and the molecular/structural recovery was inspected. The procedure was repeated 6 times in a cyclic way. Another set of samples was subjected to the same protocol, with occurrence of the rDA reaction at 120 °C.
- Instrumented microscratches of 50 μm length were performed with a Universal Nanomechanical Tester (UNAT) Asmec. During the test, a diamond spherical tip (with a radius of 7.53 μm) moved laterally over the surface while a normal force of 20 mN was applied. Tangential forces and normal displacements were registered. Pre- and postscratch inspections were carried out, in order to obtain proper cross-section profiles before and after the healing procedure. Scratches were repeated at least four times in different locations of the samples.
- Controlled macro-scratches (>2 cm) were performed by sliding a razor blade oriented at 45° to the PU surface, with a motorized constant rate. No additional normal force was applied. The scratch widths are almost similar for all the samples along their lengths.
- According to the ultimate elongation results of each PU composition, a large tensile deformation was applied. After a minimal instantaneous elastic recovery, a second shape was fixed.

Experimental healing conditions were chosen to optimize the reversibility and shape memory ability of the system in the same heating procedure at 50 °C. Functional and structural healing evolution was followed in time by means of different techniques:

- Structural/molecular recovery monitoring was performed by ATR-FTIR, as mentioned before. Typical maleimide peaks at 690 and 828 cm^{-1} [29] provided good qualitative online profiles of the DA adducts break and reformation. Results were correlated with the evolution of the characteristic "furan breathing" signal at 1012 cm^{-1}, typical for oxirane rings.[30]
- In situ images were recorded just after performing the microscratches, and after different healing times at 50 °C, with scanning probe microscopy. Profiling of the pictures with a whitelight confocal microscope μSurf (Nanofocus) was conducted after scratching and healing, for an accurate evaluation of the scratch groove's evolution.
- Scanning electronic microscopy (SEM) was used for the macro-scratches inspection after 1 and 7 days of healing, in a SEM Quantafeg, FEI equipment. Samples were previously covered by a 300 Å gold layer. An optical microscope with a heating plate was also used for sample monitoring.
- The evolution of the mechanical properties of a set of samples of each composition was evaluated during healing at 50 °C. After 1, 7, and 14 days, a minimal of three samples were cooled down to room temperature each time, in order to allow PCL crystallization before tensile testing. The same large tensile deformation previously applied to the original samples was once again implemented to the healed specimens. Two similar cycles were consecutively conducted.

■ RESULTS AND DISCUSSION

A furan-containing diol (FD) was successfully synthesized by a straightforward thiol–ene reaction after which no further purification was needed. The chemical structure and purity were confirmed by ^1H NMR (Figure S1) and LC-MS.

In the same reaction vessel, PUs were prepared through the two-step strategy schematized in Figure 2 and detailed in the Experimental Section. First, a tetraol containing two furan-maleimide adducts is prepared after which PCL diol, in combination with HDI and a catalyst, is added to the vessel and reacted at different temperature conditions (Figure 2).

dx.doi.org/10.1021/ma402471c | *Macromolecules* XXXX, XXX, XXX–XXX

Thermo-Reversibility. The Diels–Alder reaction between the synthesized FD and mM was first evaluated at 40 °C, with the purpose of assigning the typical NMR signals of the main functional groups from this model reaction. The absence of aromatic signals in mM provided clearer spectra and facilitated the interpretation. Spectra and kinetics of this model reaction are available in the Supporting Information (Figure S2). As expected, PUs prepared with mM had no structural integrity, given that multifunctional maleimides are required.

In the first part of the research, the DA forward reaction among FD and bM was optimized. The effect of temperature on the reaction rate and conversion is shown in Figure 3. Best

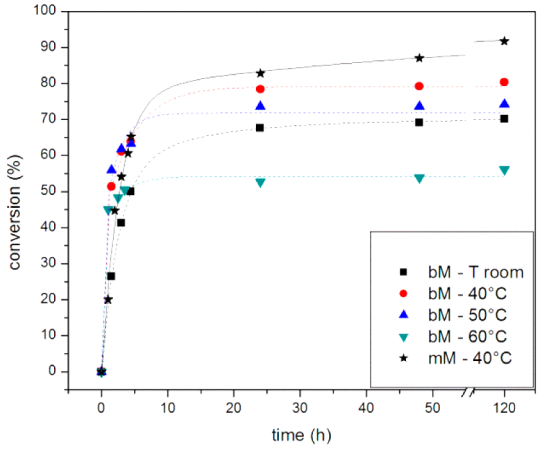

Figure 3. Effect of temperature on the DA reaction rate among FD and bM. The reaction of FD with mM is included for comparison purposes.

conversions were obtained at 40 °C with a minimal reaction time of around 12 h. Longer reaction times would only increase the exo/endo ratio of the resulting adducts.[31] A higher conversion was reached when mM is used instead, probably due to the higher mobility of the monofunctional maleimide. It is worth noting that the reaction successfully proceeded at room temperature with only a slightly lower yield.

FTIR spectra confirmed the thermo-reversibility of the Diels–Alder adducts. Any side reaction that causes furan ring-opening was discarded, both in the reaction media and in presence of the PU catalysts. The "furan breathing" peak[30] at 1012 cm^{-1} persisted, due to the furan rings remaining unreacted until the Diels–Alder reaction with maleimide groups.

For the same system, the effect of temperature and time on the retro-DA reaction (rDA) was also studied. Figure 4 shows the yields of the rDA, generating free furan/maleimide moieties under different experimental conditions, and the DA recovery at 40 °C. In all cases, the conversion was calculated by NMR, based on the remaining product of the previous state. Temperatures higher than 90 °C and long reaction times favored the rDA reaction.

Reversibility was proven in a cyclic way by ^{1}H NMR, at 40 °C for forward-DA and 100 °C for rDA reactions. Despite the fact that the equilibrium is not shifted completely, as earlier observed by Bowman,[32] the characteristic signal evolution was clear (Figure S3). The furan signals disappeared almost completely after the DA reaction at 40 °C but were recovered after rDA, also after the third cycle. The maleimide signals

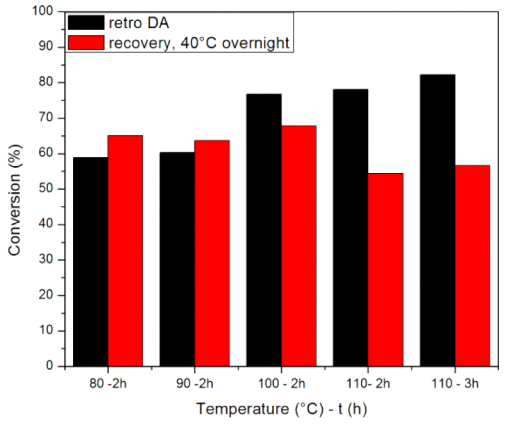

Figure 4. Effect of temperature on the rDA reaction and the first cycle of DA recovery.

partially overlapped with the aromatic ones, thus they were not appropriate for conversion calculations.

In the next step of the research, this DA system was applied for the synthesis of PCL-containing PUs as outlined in Figure 2 and detailed in the Experimental Section.

Characterization of Polyurethanes. Tough, flexible PUs were obtained as 1,5 mm thick sheets. The variation of the hard segment content resulted in materials with different cross-linking degrees, as evidenced by TGA and DMA. As expected, materials with higher amount of cross-linkers (PU-50s) exhibited the highest residual mass and the lowest degradation rate. Indeed, the first derivative of the thermogravimetric curve (DTG) showed a maximal degradation rate around 370 °C in all cases, but the height of the DTG peak showed a decreasing trend with increasing HS content (Figure S4). The same trend was observed for the storage modulus in the rubber state, which was almost quadrupled when increasing the HS content from 15 to 50% (Table S1). This fact is in accordance with the increase of the cross-linking degree.

Three main thermal transitions could be distinguished by DSC (Figure S5), with temperatures independent of the type of catalyst (Zr- or Sn-based). A first endothermic peak around 50 °C encompassed both the PCL melting together with the DA reaction, and it appeared at a slightly lower temperature in the materials with a higher HS content. The melting point and temperature range of the PCL semicrystalline (soft) segments depend on the hard/soft segment contents of PU.[21] Accordingly, the melting point of the PCL segments in PU decreases with increasing hard segment content because both the crystallization of the hard segments and the cross-linking process of the PU chains by Diels–Alder bonds interfere with the crystallization of the PCL segments. Another endotherm around 100 °C was assigned to the rDA reaction.[11,33] Its area increased with the HS content, while it could not be distinguished for PU-15T, most likely as a result of the lower amount of DA adducts present in this composition. In the cooling scan, the exothermic peaks related to the PCL crystallization showed a large decreasing trend for its temperature maximum when increasing the hard segment content, i.e. the DA cross-linker amount. This fact showed the great influence of the HS content on the material's semi-crystallinity at room temperature. A large quantity of cross-links can indeed hinder the crystallization because of hindered polymer chain alignment. The resulting highly cross-linked material is in that case more amorphous with higher

dx.doi.org/10.1021/ma402471c | Macromolecules XXXX, XXX, XXX–XXX

transparancy, but still maintains the PCL shape memory effect. As a consequence, large differences in the materials opacity can be noted in Figure 5.

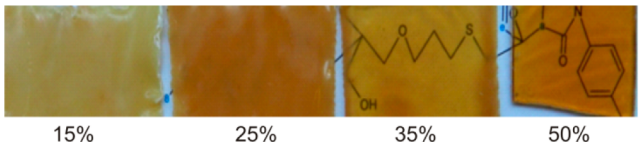

Figure 5. Photographs of PU-Zs prepared with different hard segment contents (HS) and put on a paper showing a chemical figure.

The resulting PUs were studied by ATR-FTIR. As observed from Figure 6, typical maleimide and furan peaks are absent in

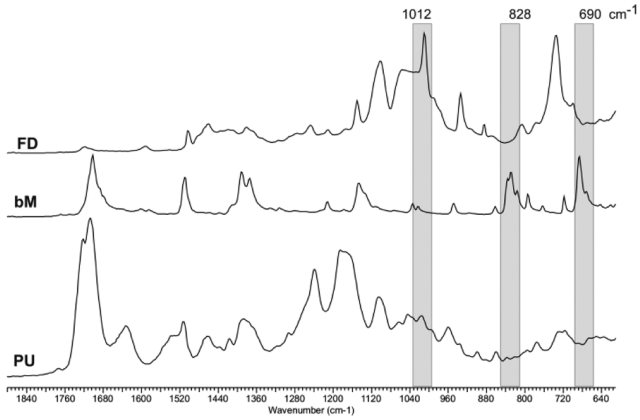

Figure 6. ATR-FTIR spectra of bM, FD, and PU-50Z.

the resulting PU. Besides, the absence of the isocyanate peak at 2270 cm^{-1} indicated that the polyurethane reaction was completed in all cases.[20]

No appreciable differences were detected between materials with different HS contents after qualitative FTIR analysis. Nevertheless, a large peak around 1631 cm^{-1} was only detected in PU-Ts (Figure S6). Given that organotin catalysts are not selective,[34] a parallel reaction among isocyanates and residual moisture is likely generating amines and CO2 as products. Indeed, even if the experimental conditions were chosen to minimize moisture in a vacuum atmosphere, a considerable higher amount of bubbles was noticed during the synthesis of PU-Ts. Further reactions of isocyanate with the formed reactive amines would lead to urea. The presence of detectable amounts of this secondary product is consistent with the carbonyl moieties observed at 1631 cm^{-1}.

Such structural differences, originating from the type of catalyst, influenced the final material properties and performance. The mechanical properties of the PUs with different compositions are shown in Figure 7. As a general tendency, with increasing HS content, a higher maximal load and stress are obtained at the expense of a reduction in the strain at break. Considerable fluctuation was found in the modulus of the materials, and it was not possible to determine a clear trend with regard to the hard segment content. In particular, significant higher maximal loads and stress were achieved with PU-Zs. Apparently, the presence of urea bonds as a secondary product in PU-Ts affected its flexibility and toughness.[35]

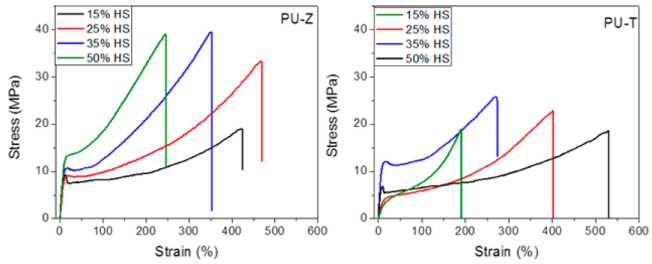

Figure 7. Typical curves obtained from the tensile test experiments for PU-Z and PU-T with different HS contents.

Healing Strategy. The shape memory recovery is the first essential task to be proven for its application as self-healing assistant. Further healing reactions would indeed not be possible unless the crack surfaces come in close proximity in a short time scale after a temperature trigger. In order to prove the shape memory effect, large tensile deformations were applied to PUs of different compositions in three consecutive cycles. The elongation parameter λ in Table 1 was defined as the ratio of the actual length over the initial sample length, i.e., $\lambda = L/L_i$. According to the ultimate elongation results of each PU composition, different large elongations were applied in each case (referred to as λ_a).

After a minimal instantaneous elastic recovery when releasing the load, a second shape was fixed (resulting shape, λ_{2°), and the recovered shape was measured (λ_{rec}) after 5 min of heating at 50 °C, above the PCL melting transition. This procedure was consecutively repeated three times. It is worth noting that for each cycle, λ_a was applied on the resulting L of the previous state, while λ_{2° and λ_{rec} were calculated with respect to the original L_i.

The results in Table 1 show that PUs with 35 and 50% of HS content showed a better fixation of the second shape (>95%). Considering that PU-15 and PU-25 showed a high elongation at break, similar to those of regular elastomeric materials, their second shape fixation was around 80%. All PUs showed excellent shape memory recoveries in the first two cycles, after large tensile deformations. After the third cycle, compositions with 15% HS presented the worst recovery yields, while PUZ-50 still performed quite good.

The maintenance of the Diels–Alder thermo-reversibility on material level is critical for the required functional performance. ATR-FTIR tests showed the occurrence of this reaction in the cured PUs. By making use of an online monitoring during several damage/healing cycles, the typical IR signals provided important structural information on the healing kinetics.

The polyurethanes were heated up to 100 °C for 1 h, and the rDA reaction was checked by the fast recovery of typical maleimide and furan peaks in the FTIR-spectra. Then, a mild heating at 50 °C progressively reformed the DA cross-linkers, as evidenced in Figure 8. Notably, the main DA recovery took place during the first hour at 50 °C. Whereas the furan peak at 1012 cm^{-1} appeared as a shoulder, the more separate maleimide peaks at 690 and 828 cm^{-1} were used for further analysis. The procedure was also performed by heating up to 120 °C, in order to prove that the partial reformation is achievable with even higher rDA yields (Figure S7). The reversible nature of the DA reaction in the PUs was successfully proven for several cycles. As expected, each cycle did not complete the Diels–Alder chemistry for 100%, but only a minimal shift of the equilibrium was noted when increasing the

dx.doi.org/10.1021/ma402471c | Macromolecules XXXX, XXX, XXX–XXX

Table 1. Shape Memory Effect of PUs with Different Compositions after Cyclic Large Tensile Deformations

			% HS			
material	cycle	$\lambda = L/L_i$	15%	25%	35%	50%
PU-Z	0	λ_o	1	1	1	1
	I	λ_a	4	3.5	2	1.75
		λ_{2°	3.22 ± 0.12	2.90 ± 0.09	1.91 ± 0.06	1.57 ± 0.08
		λ_{rec}	1.02 ± 0.01	1.00 ± 0.00	1.01 ± 0.01	1.01 ± 0.01
	II	λ_a	4	3.5	2	1.75
		λ_{2°	3.39 ± 0.09	3.16 ± 0.55	1.92 ± 0.08	1.75 ± 0.05
		λ_{rec}	1.06 ± 0.02	1.04 ± 0.01	1.05 ± 0.05	1.07 ± 0.06
	III	λ_a	4	3.5	2	1.75
		λ_{2°	4.16 ± 0.12	nd[a]	1.96 ± 0.09	1.79 ± 0.10
		λ_{rec}	2.48 ± 0.10	nd[a]	1.09 ± 0.12	1.10 ± 0.09
PU-T	0	λ_o	1	1	1	1
	I	λ_a	4	3.5	2	1.75
		λ_{2°	3.31 ± 0.16	3.12 ± 0.19	1.94 ± 0.13	1.75 ± 0.08
		λ_{rec}	1.02 ± 0.01	1.03 ± 0.01	1.05 ± 0.05	1.04 ± 0.03
	II	λ_a	4	3.5	2	1.75
		λ_{2°	3.45 ± 0.05	2.90 ± 0.10	2.17 ± 0.08	1.78 ± 0.04
		λ_{rec}	1.06 ± 0.04	1.12 ± 0.09	1.10 ± 0.06	1.00 ± 0.01
	III	λ_a	4	3.5	2	1.75
		λ_{2°	4.23 ± 0.10	nd[a]	2.26 ± 0.15	nd[a]
		λ_{rec}	2.59 ± 0.09	nd[a]	1.13 ± 0.10	nd[a]

[a]Break of the specimens did not allow an accurate measurement.

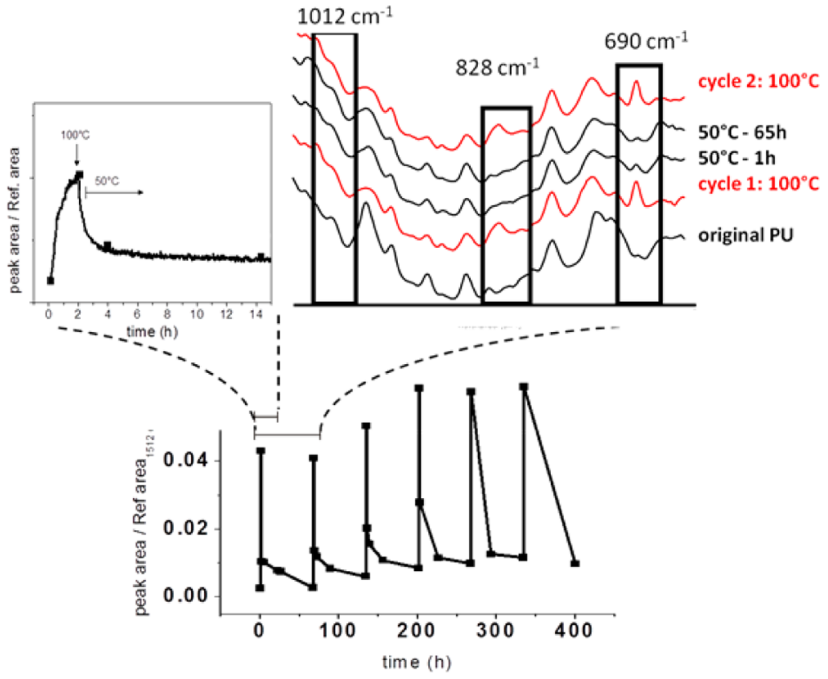

Figure 8. FTIR normalized area of the 690 cm^{-1} maleimide band during six reaction cycles. Samples were heated up to 100 °C for 1 h (rDA), and later healed at 50 °C (DA) for 65 h in each cycle. Enlarged: Spectra and online FTIR profile of the peak evolution during the first thermal cycle.

number of cycles (Figure 8, bottom part). This fact assures the material thermo-reversibility, which is a critical feature in the proposed healing strategy.

Healing Behavior under Mild Conditions. Cuts on a macro-scale were manually applied on the PU materials with a razor blade, Figure 9a) shows the aspect of PU-50Z before and after 24 h of healing at 50 °C, inspected with an optical microscope. The SEM images of a similar scratch in the same sample are shown in Figure 9b). No significant differences were found when heating at 50 °C for a maximum of 7 days. An alternative healing procedure tested the effect of 1 h of heating at 100 °C, previous to the healing procedure at 50 °C. This promotion of rDA would purposely break more adducts, so that DA rearrangement would occur in a more efficient way. However, results in Figure 9b.iii showed only a slight improvement in the scars.

Beyond simply testing the recovery capability by 2D visual methods to confirm the fundamental role of DA bonds, the application of nanoscratch techniques allowed the identification of the main factors involved in the healing procedure (Figure

dx.doi.org/10.1021/ma402471c | Macromolecules XXXX, XXX, XXX−XXX

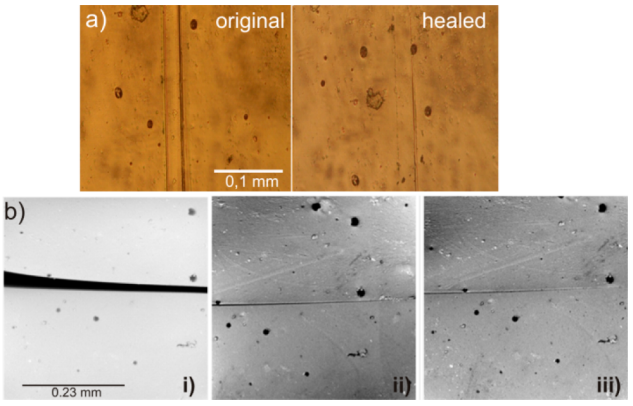

Figure 9. (a) Optimal microscopy of the PU-50Z sample cut with a razor blade before (left) and after (right) healing at 50 °C for 24 h. (b) SEM images of (i) the original scratch, (ii) scratch after healing at 50 °C for 24 h, and (iii) scratch after heating at 100 °C for 1 h and then healing for 24 h at 50 °C.

10). A further optimization required an in-depth study of the influence of the hard segment content, the nature of the catalysts and the matrix elasticity. Knowledge on those structure−property relationships is the key to improve the material design for enhancing the functional performance.

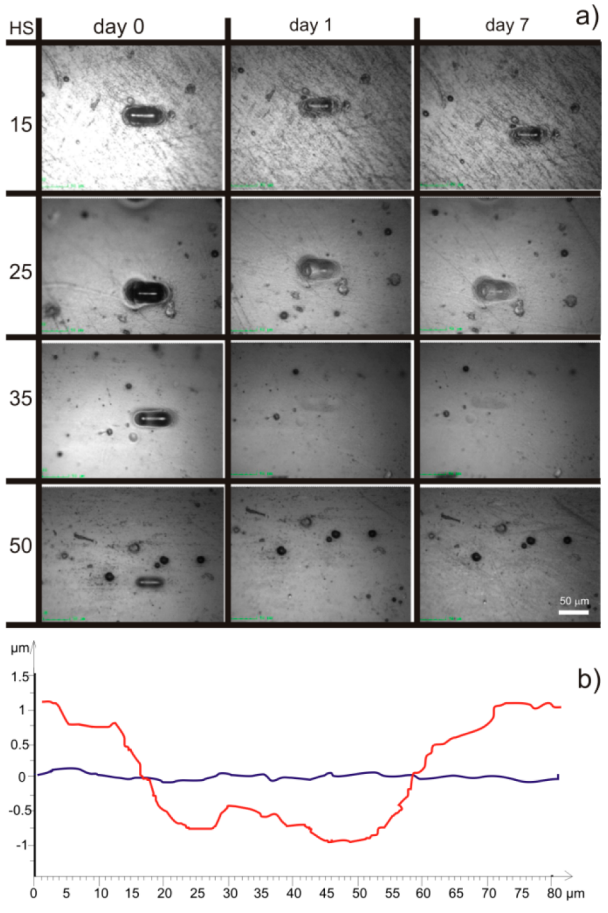

Figure 10. (a) Pictures of 50 μm scratches performed with 20 mN of normal load in PUs-Z of different HS contents: just after performing the scratch (original), after 24 hs (day 1) and seven days (day 7) of healing at 50 °C. (b) Profiling of PU-50Z scratch image, before (red) and after (blue) healing at 50 °C for 24 h.

Instrumented indentations assured the application of an identical damage to all PUs, so that direct comparison of the polymer deformation near the surface was possible. Purely elastic responses were avoided by using different normal forces to confirm the trends.

Pictures of the original scratches showed a "pile up" effect as a consequence of the plastic deformation induced by the tip. This accumulated material was restored in all cases after exposure at 50 °C as a consequence of the shape memory effect. After 24 h, scratches were completely healed in PU-50Z, while only a slight mark was detectable in PU-35Z. The same behavior was observed for the PU-T counterparts. A section profile of a scratch in sample PU-50Z before and after healing at 50 °C (Figure 10b) evidenced a 3D recovery in surface and in depth. Nevertheless, although PU-15 and PU-25 showed a more elastic behavior (Table 1 and Figure 7), they did not remend the scratches after healing at 50 °C. This fact suggested a nonelastic recovery of the scratches and supported the healing strategy based on DA bond reformation. Indeed, healing was only effective in PU-materials with a higher HS content, i.e., more DA cross-linkers in their composition. It is worth noting that no appreciable differences were detected between healing for 1 or 7 days, in accordance with the observed DA recovery kinetics in the PUs.

Functional Mechanical Healing. The ultimate objective of self-healing implies an extension of the material life in service. Further than an esthetical issue, an actual healing requires functional recovery. Therefore, the mechanical properties were evaluated after similar large elongation cycles compared to those described in Table 1. PU-15s were excluded from the analysis because of their non- adequate cyclic shape memory effect and the lower DA cross-linker content.

The first cycle in Table 2 allowed for the comparison of the original material properties (day 0) before the first elongation cycle, with those resulting after 1 and 7 days of heating at 50 °C. In general, the elastic modulus (E) decreased after large deformations but it was experimentally not possible to show that DA adducts (weakest bonds) were actually broken during the tensile test. Nevertheless, after seven days of healing E was recovered or even increased. The procedure was repeated in cycle II by the application of the same tensile strain to the already "healed" specimens, and the subsequent heating at 50 °C for 7 more days. Again, the moduli increased in all compositions. This behavior can be related to the progressive chain rearrangements after application of the repetitive large elongations. Indeed, a better polymer chain alignment may allow for more effective DA reformation reactions, thus the network can be evenly more cross-linked. The loss of flexibility influences the elastic and ductile behavior, leading to a more brittle material with higher modulus. The ultimate strain (ε) at break decreased with the number of cycles, as shown in Table 2, but the maximal force (P) and stress (σ) did not show large variations (Figure S8).

System Versatility. The proposed strategy outlined before was proven and optimized for a PU- material composed of FD and bM. From this study, it was determined that a sufficient amount of DA cross-linkers is required for healing. Both PU-35 and PU-50 were optimal materials with remendable features at very mild conditions, although interesting differences in their properties were detected. The objective of this section is to show the even larger versatility of this new self-healing strategy. Indeed, depending on the desired applications, materials can be tuned to have diverse optical, physical and mechanical

dx.doi.org/10.1021/ma402471c | *Macromolecules* XXXX, XXX, XXX−XXX

Table 2. Evolution of the Mechanical Properties after Several Elongation/Healing Cycles

			25% HS		35% HS		50% HS	
	cycle	days	Z	T	Z	T	Z	T
E (MPa)	I	0	159 ± 18	152 ± 22	118 ± 22	119 ± 33	81 ± 26	75 ± 19
		1	114 ± 2	103 ± 8	100 ± 18	124 ± 28	50 ± 11	55 ± 5
		7	126 ± 23	123 ± 24	138 ± 21	146 ± 19	127 ± 10	148 ± 27
	II	14	141 ± 34	179	177 ± 15	246 ± 27	214 ± 28	270 ± 18
ε (%)	I	0	536 ± 82	335 ± 61	313 ± 10	264 ± 25	264 ± 28	202 ± 28
		1	471 ± 83	384 ± 58	314 ± 20	336 ± 36	314 ± 19	213 ± 25
		7	392 ± 115	296 ± 38	237 ± 12	255 ± 21	237 ± 12	178
	II	14	316 ± 19	235	161	233	161	150

properties, by the modification of the monomer structures (examples in Table S2). Both the DA kinetics and the polyurethanes final properties were notably affected when the furan or maleimide groups are included in the polymer backbone instead of being pendant ones, or when a different switching segment is used (see Supporting Information). All the studied alternative systems showed already an excellent shape memory effect and a certain healing efficiency. Nevertheless, the latter can be optimized based on the previous conclusions regarding the optimal HS content and catalysts.

CONCLUSIONS

Tough, flexible and transparent polyurethane networks with healing capability at mild temperature conditions were successfully prepared in a one-pot procedure. Remendability was achieved by combining the occurrence of two processes at 50 °C: a fast shape memory effect brought the free furan and maleimide moieties together, after which a progressive Diels–Alder reaction could reform the covalent bonds on a longer time scale. The multihealing strategy was systematically verified and trends regarding the compositions and the role of each component were clarified.

The hard segment content does not only affect the physical/structural parameters such as crystallinity, toughness and transparency but also the self-healing characteristics in accordance with the final cross-linking degrees. The Diels–Alder moieties were proven to be the most critical factor for the thermo-remendability. Formulations with a higher hard segment content generated transparent materials with the best healing behavior. No flow or complete melting of the sample was required for this healing process, and the structural integrity was practically unaffected. It should be emphasized that the DASMASH synergic combination foresees the possibility of healing large damaged areas.

ASSOCIATED CONTENT

Supporting Information

^{1}H NMR spectra of the raw materials synthesized, the model reactions and the DA required for the polyurethane synthesis, full characterization of the polyurethanes (TGA, DMA, DSC, FTIR) with different compositions, experimental details about the additional networks prepared to prove the strategy versatility. This material is available free of charge via the Internet at http://pubs.acs.org.

AUTHOR INFORMATION

Corresponding Author

*(F.E.D.P.) Fax: (+32)92644489. Telephone: (+32)92644503. E-mail: fillip.duprez@ugent.be.

Present Address

[§]Faculty of Materials Technology, Ho Chi Minh City University of Technology, Vietnam National University, 268 Ly Thuong Kiet, 10 District, Ho Chi Minh City, Vietnam.

Notes

The authors declare no competing financial interest.

ACKNOWLEDGMENTS

G.R. thanks the EuroTango II Project–Erasmus Mundus Programme and the Consejo Nacional de Investigaciones Científicas y Técnicas (CONICET) for financial support. X.K.D.H. thanks the Strategic Initiative Materials (SIM) project, supported by the Agency for Innovation through Science and Technology (IWT), for a doctoral fellowship. F.E.D.P. acknowledges the Belgian Program on Interuniversity Attraction Poles initiated by the Belgian State, the Prime Minister's office (P7/05) and the European Science Foundation–Precision Polymer Materials (P2M) program for financial support.

REFERENCES

(1) Billiet, S.; Hillewaere, X. K. D.; Teixeira, R. F. A.; Du Prez, F. E. *Macromol. Rapid Commun.* **2013**, *34*, 290–309.
(2) Williams, K. A.; Dreyer, D. R.; Bielawski, C. W. *MRS Bull.* **2008**, *33*, 759–765.
(3) Murphy, E. B.; Wudl, F. *Prog. Polym. Sci.* **2010**, *35*, 223–251.
(4) Chung, C.-M.; Roh, Y.-S.; Cho, S.-Y.; Kim, J.-G. *Chem. Mater.* **2004**, *16*, 3982–3984.
(5) Ghosh, B.; Urban, M. W. *Science* **2009**, *323*, 1458–1460.
(6) Froimowicz, P.; Frey, H.; Landfester, K. *Macromol. Rapid Commun.* **2011**, *32*, 468–473.
(7) Scott, T. F.; Schneider, A. D.; Cook, W. D.; Bowman, C. N. *Science* **2005**, *308*, 1615–1617.
(8) Nicolaÿ, R.; Kamada, J.; Van Wassen, A.; Matyjaszewski, K. *Macromolecules* **2010**, *43*, 4355–4361.
(9) Amamoto, Y.; Kamada, J.; Otsuka, H.; Takahara, A.; Matyjaszewski, K. *Angew. Chem., Int. Ed.* **2011**, *50*, 1660–1663.
(10) Gyarmati, B.; Némethy, Á.; Szilágyi, A. *Eur. Polym. J.* **2013**, *49*, 1268–1286.
(11) Chen, X.; Dam, M. A.; Ono, K.; Mal, A.; Shen, H.; Nutt, S. R.; Sheran, K.; Wudl, F. *Science* **2002**, *295*, 1698–1702.
(12) Laita, H.; Boufi, S.; Gandini, A. *Eur. Polym. J.* **1997**, *33*, 1203–1211.
(13) Watanabe, M.; Yoshie, N. *Polymer* **2006**, *47*, 4946–4952.
(14) Zhang, Y.; Broekhuis, A. A.; Picchioni, F. *Macromolecules* **2009**, *42*, 1906–1912.
(15) Chen, X.; Wudl, F.; Mal, A. K.; Shen, H.; Nutt, S. R. *Macromolecules* **2003**, *36*, 1802–1807.
(16) Tian, Q.; Yuan, Y. C.; Rong, M. Z.; Zhang, M. Q. *J.Mater. Chem.* **2009**, *19*, 1289–1296.
(17) Bai, N.; Saito, K.; Simon, G. P. *Polym. Chem.* **2013**, *4*, 724–730.

(18) Gaina, C.; Ursache, O.; Gaina, V. *Polym. Plast. Technol.* **2011**, *50*, 712−718.
(19) Hearon, K.; Gall, K.; Ware, T.; Maitland, D. J.; Bearinger, J. P.; Wilson, T. S. *J. Appl. Polym. Sci.* **2011**, *121*, 144−153.
(20) Sivakumar, C.; Sultan Nasar, A. *J. Appl. Polym. Sci.* **2011**, *120*, 725−734.
(21) D'Hollander, S.; Van Assche, G.; Van Mele, B.; Du Prez, F. *Polymer* **2009**, *50*, 4447−4454.
(22) D'Hollander, S.; Gommes, C. J.; Mens, R.; Adriaensens, P.; Goderis, B.; Du Prez, F. *J. Mater.Chem.* **2010**, *20*, 3475−3486.
(23) Defize, T.; Riva, R. l.; Raquez, J.-M.; Dubois, P.; Jérome, C.; Alexandre, M. l. *Macromol. Rapid Commun.* **2011**, *32*, 1264−1269.
(24) Raquez, J.-M.; Vanderstappen, S.; Meyer, F.; Verge, P.; Alexandre, M.; Thomassin, J.-M.; Jérôme, C.; Dubois, P. *Chem.—Eur. J.* **2011**, *17*, 10135−10143.
(25) Oya, N.; Saitoh, S.; Furuhashi, Y.; Yoshie, N. *J. Polym. Sci., A: Polym.Chem.* **2012**, *50*, 1926−1932.
(26) Mallek, H.; Jegat, C.; Mignard, N.; Abid, M.; Abid, S.; Taha, M. *J. Appl. Polym. Sci.* **2012**, *129*, 954−964.
(27) Rodriguez, E. D.; Luo, X.; Mather, P. T. *ACS Appl. Mater. Interfaces* **2011**, *3*, 152−161.
(28) Luo, X.; Mather, P. T. *ACS Macro Lett.* **2013**, 152−156.
(29) Grenier-Loustalot, M.-F.; Gouarderes, F.; Joubert, F.; Grenier, P. *Polymer* **1993**, *34*, 3848−3859.
(30) Derrick, P. J.; Åsbrink, L.; Edqvist, O.; Lindholm, E. *Spectrochim. Acta A* **1971**, *27*, 2525−2537.
(31) Cooley, J. H.; Williams, R. V. *J. Chem. Educ.* **1997**, *74*, 582.
(32) Bowman, C. N.; Kloxin, C. J. *Angew. Chem., Int. Ed.* **2012**, *51*, 4272−4274.
(33) Scheltjens, G.; Diaz, M. M.; Brancart, J.; Van Assche, G.; Van Mele, B. *React. Funct. Polym.* **2013**, *73*, 413−420.
(34) Blank, W. J.; He, Z. A.; Hessell, E. T. *Prog. Org. Coat.* **1999**, *35*, 19−29.
(35) Yi, J.; Boyce, M. C.; Lee, G. F.; Balizer, E. *Polymer* **2006**, *47*, 319−329.